



Automated SEM-EDS mineralogical characterisation of archaeological pottery from Luxmanda and Mumba Rockshelter, Tanzania

Titus Luomba Ombori^{a,*}, Duncan Pirrie^b, Matthew R. Power^c, Ian Skilling^b, Agness O. Gidna^d, Audax Z.P. Mabulla^e, Pastory M. Bushozi^e, Mary E. Prendergast^f, Katherine M. Grillo^g

^a Department of History, Political Sciences & Development Studies, University of Dar es Salaam (MUCE), Iringa, P.O Box 2513, Tanzania

^b Faculty of Computing, Engineering and Science, University of South Wales, Pontypridd CF37 4BD, UK

^c Vidence Inc., 4288 Lozells Avenue, Suite 213L, Burnaby, British Columbia V5A 0C7, Canada

^d Ngorongoro Conservation Area Authority, Tanzania

^e Department of Archaeology and Heritage, University of Dar es Salaam, PO Box 35050, Dar es Salaam, Tanzania

^f Department of Anthropology, Rice University, Houston, TX 77251, USA

^g Department of Anthropology, University of Florida, 1112 Turlington Hall, PO Box 117305, Gainesville, FL 32611-7305, USA

ARTICLE INFO

Keywords:

Pastoralism

Tanzania

Raw material provenancing

ABSTRACT

This study presents the first application of automated scanning electron microscopy with linked energy dispersive spectrometry (SEM-EDS) to characterise “Narosura” Pastoral Neolithic (PN) pottery from the Luxmanda site in northern Tanzania. Additional samples from Mumba Rockshelter in the Eyasi Basin are also presented for comparison. The PN period in eastern Africa (~5000–1200 BP) was characterised by the spread of domestic livestock and new forms of material culture associated with pastoralism. Despite extensive pottery macro-typological analysis in this region, few studies have focused on the mineralogical composition and provenance of the raw materials for PN pottery production. By examining 13 pottery samples using automated SEM-EDS, this study has identified four distinct mineralogical groups, each of which reflect the localised sourcing of raw materials for ceramic manufacture. The findings reveal differences in raw material sources suggesting varying pottery production techniques and cultural practices.

1. Introduction

The Pastoral Neolithic (PN) in eastern Africa was a long and complex period that lasted from approximately 5000 BP to 1200 BP. It marks the first transition from hunting and gathering to food production in the region, which took the form of pastoralism, or the herding and management of livestock including cattle, sheep and goats (Bower, 1991; Robertshaw, 2021; Ombori, 2024). Zooarchaeological research documents the emergence of specialized pastoralist economies after c. 3300 BP at sites stretching from central Kenya through northern Tanzania (Gifford-Gonzalez, 1998; Marshall, 1990; Prendergast et al., 2019a), although some PN sites also attest to hunting and/or interaction with foragers (Gifford et al., 1980; Prendergast, 2011). Whether herders also cultivated domestic crops is unknown (Robertshaw, 2021). These specialised pastoralists used pottery (Ashley and Grillo, 2015) and blade-based lithic technologies, including obsidian tools (Goldstein, 2018).

Different material culture traditions (broadly labelled “Elmenteitan” and “Savanna Pastoral Neolithic” or SPN) have been identified within the PN (Ambrose, 1984). While Elmenteitan sites (concentrated in southwestern Kenya) and SPN sites (found from central Kenya through northern Tanzania) can be differentiated on the basis of material culture and preferred obsidian sources, genetic data show no distinctions among these PN communities (Prendergast et al., 2019b).

Archaeologists studying the PN have previously used macro-typological analyses for pottery (description and classification based on characteristics such as decorative techniques and motifs, firing conditions, and vessel shapes). Various typological schemes have been proposed for PN ceramics; Wandibba’s (1980) system identifying “Nderit” ware, “Narosura” ware, “Remnant” ware (now typically referred to as “Elmenteitan” ware), “Maringishu” ware, and “Akira” ware is most commonly employed today (see also Collett and Robertshaw, 1983; Ashley and Grillo, 2015; Grillo et al., 2022; Ombori, 2024).

* Corresponding authors at: University of Dar es Salaam, Tanzania (T.L. Ombori). University of Florida, USA (K.M. Grillo).

E-mail address: titus.ombori@udsm.ac.tz (T.L. Ombori).

However, there have been very few attempts to characterise the composition of PN pottery to understand manufacturing technologies, firing methods, tempering practices, and possible provenance of the raw materials, with studies to date mainly based on thin-section petrography (Langdon and Robertshaw, 1985; Ombori, 2021). Studies of PN ceramic use have likewise been rare; Grillo et al.'s (2020) study of lipid residues in PN ceramics provided direct evidence that pots were used for processing livestock carcasses, milk, and plants. As herding became increasingly specialized throughout the Rift Valley, pots were intensively used to process livestock carcasses into meat/fat/bone soups.

Despite a dearth of research thus far into PN ceramic production and use, we argue that understanding whether or not ceramics were being locally produced and used, for example, has broader significance in terms of how we conceptualize pastoralist lifeways and relationships between patterns of mobility, craft production, and the circulation of material goods across physical and social landscapes. Indeed, as Klehm et al. (2023) point out in their sourcing study of PN stone beads in the Turkana Basin, what "local" means for ostensibly mobile populations can be a complicated question. Langdon and Robertshaw's (1985) study of Elmenteitan, Narosura, Akira, and Early Iron Age pottery in southwestern Kenya used petrography and X-ray fluorescence to determine that those ware types were produced with clays and paste recipes easily distinguishable from each other. Potters almost always chose clay, though, very local to the sites where the broken pots were eventually discarded. Akira ware seems to be the exception, lending to support of the idea that those pots were exchanged within farther-reaching social networks. There is otherwise no evidence, in this part of southwest Kenya, for long-distance movement of clays or pots themselves. While some degree of mobility may have been important for PN livestock management (Janzen et al., 2020), and PN material culture exchange is well attested in obsidian circulation (Merrick and Brown, 1984), ceramic production and circulation appears to have been grounded largely in place.

Increasingly, to understand the provenance of the raw materials used in archaeological ceramics optical microscopy has been integrated with a range of other mineralogical and chemical analytical tools (e.g. Knappett et al., 2011; Ogalde et al., 2021; Quinn, 2013; Quinn et al., 2020) such as automated scanning electron microscopy coupled with energy dispersive spectrometry (automated SEM-EDS), X-ray fluorescence (XRF), X-ray diffraction (XRD), neutron activation analysis (NAA) and laser ablation-inductively coupled plasma mass spectrometry (LA-ICP-MS) (e.g. Glascock and Neff, 2003; Peacock et al., 2007; West et al., 2016; Quinn, 2013; 2020; 2022). Automated SEM-EDS analysis has been applied to studies of archaeological ceramics from a wide range of sites (e.g. Knappett et al., 2011; Hillditch et al., 2012, 2016; Kelly et al., 2014; Menzies et al., 2015; Šegvić et al., 2016; Frigóle et al., 2019; Derenne et al., 2020; Carloni et al., 2021, 2022).

Despite the adoption of automated SEM-EDS analysis in archaeological ceramic analysis, in Africa the potential of this method is still under-utilised. Thus, the application of automated SEM-EDS to PN pottery from eastern Africa is particularly significant as ceramic macro-typological analysis dominates archaeological research for this time-frame, yet identifying the sources of pottery raw materials is relevant to understanding pastoralist social networks and interactions.

In this paper, we present a pilot study, characterising a suite of Narosura pottery samples collected from the Luxmanda site on the Mbulu Plateau in Tanzania (Prendergast et al., 2013; Grillo et al., 2018). Additional ceramic samples from the multicomponent site of Mumba Rockshelter, in the Eyasi Basin, Tanzania (Bushozi et al., 2020; Mwitondi and Bushozi, 2024), are also presented for comparison. This paper expands on Ombori's (2021) doctoral research, which used petrographic and manual SEM-EDS methods to examine pottery from two locales in north-central Tanzania. Ombori (2021) indicated that vessels at the Luxmanda site on the Mbulu Plateau were likely made from clay sourced from the immediate region, but intriguingly suggested that pottery from Mbulu Plateau may also have been acquired and used by PN

communities living in the Eyasi Basin to the north. This paper presents automated SEM-EDS analysis of sherds originally analysed with petrographic methods in Ombori (2021).

This paper is the first published application of automated SEM-EDS analysis to ceramics in eastern Africa. Detailed mineralogical characterisation allows the identification and classification of minerals at the microscale, enabling detailed study of the clay matrices and non-plastic inclusions within the ceramics. We present this study as an initial way to identify knowledge and use of raw material sources by a PN community in a geologically diverse region, gleaning new information from a small sample of Narosura ceramics into how pastoralists incorporated ceramic production, and potentially exchange, into their lives.

2. Archaeological and geological context of study area

2.1. Narosura ware in broader context

Narosura ware, first defined at the type site in southern Kenya by Odner (1972), is one of several ceramic wares considered part of the SPN material tradition (Ambrose, 1984). It was described as typically having comb-stamped or incised designs in bands immediately below rims. Those bands are often bordered by comb-stamped or incised horizontal lines, and several decorative motifs within bands occur, including zig-zags. Forms are typically narrow-mouthed bowls, bowls with slightly everted rims, and beaker-like vessels. Narosura ware is reported at sites spanning the terminal fourth through early second millennia BP in central and southern Kenya and parts of Tanzania. In Tanzania, Narosura ware has been documented in the Serengeti (Mehlman, 1989), Eyasi Basin (Prendergast, 2008), Mbulu Plateau (Grillo et al., 2018), West Kilimanjaro (Mturi, 1986), and possibly at the coast (Chami and Kwekason, 2003). This wide distribution raises questions about the typological variants of Narosura pottery (Ombori, 2024), and about the social networks among pastoralists that may have supported the exchange of ideas and/or materials for the production of this ware.

2.2. Luxmanda, Mbulu Plateau

The Luxmanda site (coordinates $-4.26, 35.32$) was discovered in 2011 (Prendergast et al., 2013) and is located near a village of the same name at the southern edge of the Mbulu Plateau, the southernmost known PN site (Fig. 1). Grillo et al. (2018) provide a detailed description of the site and its associated artefacts. It is the largest intact PN occupation site found to date in eastern Africa. Radiocarbon dates on charcoal, bone, and organic material in ceramics centre around c. 3000 cal BP, showing that Luxmanda is amongst the earliest of the currently dated sites with SPN material culture. Faunal remains attest to specialized pastoralism (Prendergast et al., 2019a). Lithics were mostly locally sourced, but obsidian was transported over c. 400 km from the Naivasha Basin in Kenya, utilizing the same sources identified at other SPN sites (Prendergast et al., 2013).

Pottery collected at the site was assigned as Narosura ware by Grillo et al. (2018). The assemblage is relatively uniform in terms of manufacture, forms, and overall style (see also Prendergast et al., 2013; Ombori, 2021). Grillo et al. (2018) noted that inclusions within the pottery included moderate to well sorted quartzose sand, and that according to local potters, the nearest clay source is near Darwedick, some 20 km from Luxmanda.

2.3. Mumba Rockshelter, Eyasi Basin

Mumba Rockshelter (coordinates $-3.54, 35.30$) is located on the northeastern margin of the Eyasi Basin in northern Tanzania (Fig. 1). The site spans c. 130,000 years of intermittent occupation, documenting early human cultural evolution and environmental interactions (e.g., Kohl-Larsen, 1943; Mehlman, 1989; Prendergast et al., 2007; Bushozi, 2023; Bushozi et al., 2020; Bader et al., 2020; Mwitondi et al., 2021).

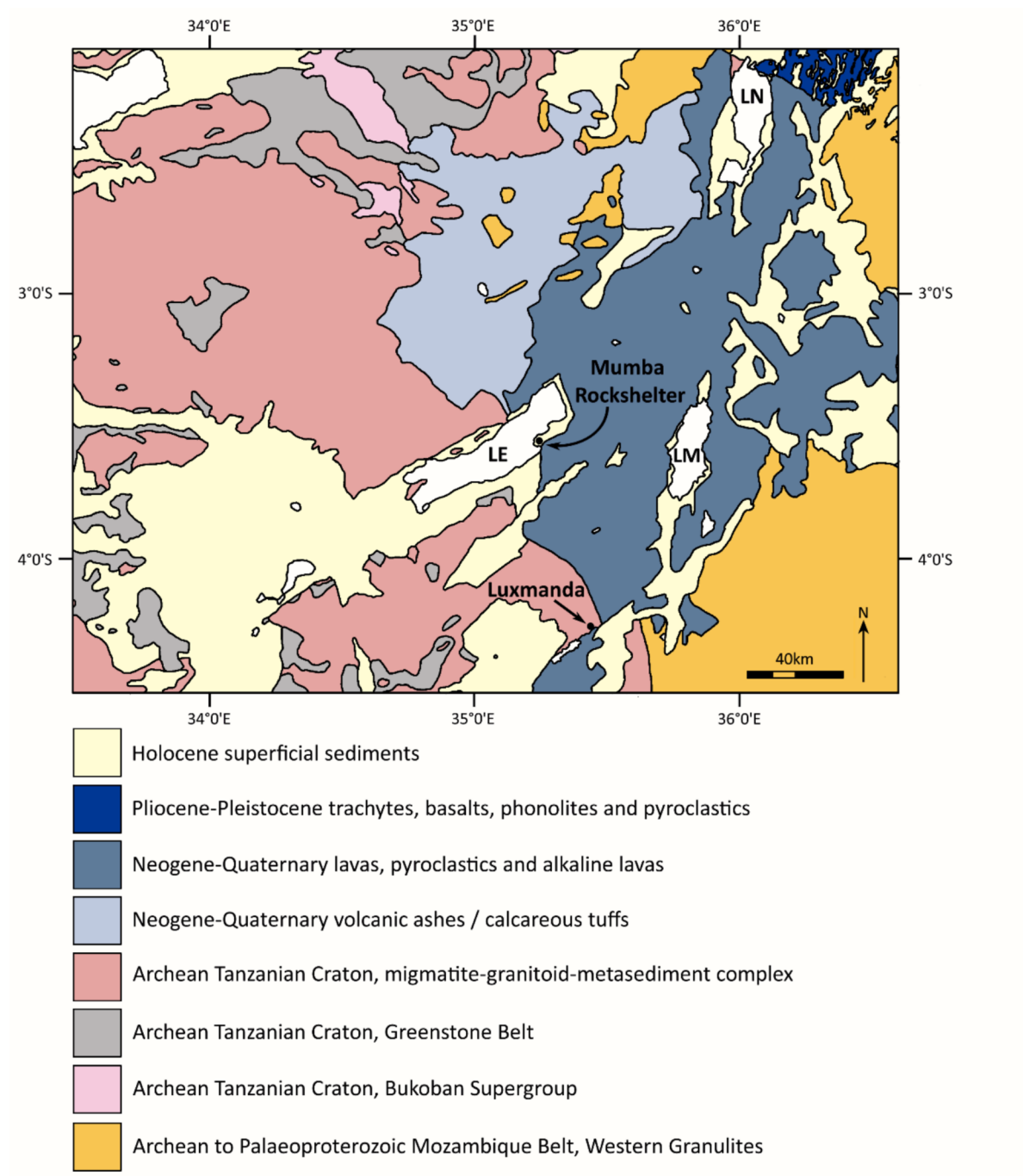


Fig. 1. Geological map showing the location of the field sites at Luxmanda and Mumba Rockshelter, Eyasi. Geological map adapted from Janzen et al. (2020). LE – Lake Eyasi, LM – Lake Manyara, LN – Lake Natron.

While most research has focused on the important Middle Stone Age (MSA) to Later Stone Age (LSA) transition and symbolic material culture (e.g., Bushozi et al., 2020; Bushozi, 2020), there are also ceramic traditions represented in the uppermost thin, poorly stratified deposits, including LSA Kansyore ware, PN Narosura ware, and Iron Age Lelesu ware (Prendergast et al., 2007; Prendergast et al., 2014).

While animal remains from Mumba are predominantly of wild fauna, indicating use of the shelter by people who were hunting, there is ample evidence from the neighbouring open-air Narosura sites for pastoralism, fishing, shellfish collection, and occasional hunting (Mehlman, 1989; Prendergast, 2011; Rubaka, 2000; Mwitondi et al., 2021; Bushozi, 2022). It thus seems plausible that Narosura ware at Mumba Rockshelter is either the product of pastoralists using the shelter, or of hunter-

gatherers in contact with these pastoralists. Ceramics identified as Iron Age were presumably produced by potters from later agricultural communities. The two ceramic sherds from Mumba analysed for this study comprise one undecorated sherd and one sherd that has an applied band with incised hatch marks. These sherds were identified by Ombori (2021) as Narosura. There is debate amongst co-authors of this paper as to attribution; some would argue that there may be a stratigraphic argument for Narosura, while others of us would consider the undecorated sherd not attributable to ware type, and the decorated sherd as either not attributable to ware type or Iron Age.

2.4. Geological setting

The Precambrian basement rocks of Tanzania are composed of the Archean Tanzanian Craton and the Archean to Mesoproterozoic Mozambique Belt (Fletcher et al., 2018; Apen et al., 2020) (Fig. 1). The Tanzania Craton is an assemblage of granite-greenstone belts formed between 2.8 and 2.6 Ga with large granitic bodies emplaced across the northern craton between 2.7 and 2.5 Ga (Apen et al., 2020). In addition, undeformed high K granites dated between 2.6 and 2.5 Ga also occur. The Neoarchean supracrustal rocks of the Tanzania Craton include chlorite schists, quartz-sericite schists, banded iron formations and hornblende gneisses, intruded by granites, diorites, syenites and gabbros (Thomas et al., 2016; Fletcher et al., 2018). Dolerite and gabbro dykes occur on the eastern margin of the Tanzanian Craton and are exposed along the margin of the Eyasi and Wembere basins (Fletcher et al., 2018). To the east of the Tanzanian Craton is the Mozambique Belt, which in northern Tanzania is divided into the Western Granulites and Eastern Granulites. The Western Granulites crop out in the study area and comprise an Archean to Palaeoproterozoic succession with garnet bearing orthogneisses and metapelites.

Cross cutting the Precambrian basement is the East African Rift System, which propagated southwards reaching northern Tanzania by about 8 Ma. In this area the East African Rift splits into three splays, the western Eyasi-Wembere Rift, the central Natron-Manyara-Balangida Rift and the eastern Pangani Rift (Ebinger et al., 1997; Ring et al., 2005) (Fig. 1). Basins developed within each of the rifts with sedimentary-volcanic infills (Fletcher et al., 2018). The contact between the Tanzania Craton and the Mozambique Belt is exposed along the uplifted flank of the Eyasi Basin (Ebinger et al., 1997).

Both Mumba Rockshelter and Luxmanda occur in the Eastern Branch of the East African Rift System in an area known as the Northern Tanzanian Divergence (NTD) (Le Gall et al., 2008; Rooney, 2020). The NTD in this area is split into two sedimentary basins, the Balangida Basin that contains the seasonal Lake Balangida, above which rises the escarpment where Luxmanda is located, and the Eyasi Basin, in which Lake Eyasi and Mumba Rockshelter are situated (Fletcher et al., 2018) (Fig. 1). Both basins began to form and fill with volcanic and sedimentary rocks about 5 Ma ago (Foster et al., 1997; Fletcher et al., 2018).

Mumba Rockshelter lies on Miocene to Recent sediments of mostly alluvial origin, but also includes associated lacustrine algal limestones, volcaniclastic deposits, salt deposits and aeolian sands (Dundas et al., 1977). Recent alluvial drainage into the site is sourced from or crosses Neoarchean age metamorphic basement rocks of the Tanzanian Craton, and Gliganic et al. (2012a, 2012b) report on dating archaeological deposits at Mumba Rockshelter based on OSL dating of detrital quartz and feldspar grains. This area of Lake Eyasi also receives drainage across volcanic rocks from the Ngorongoro Volcanic Highlands (NVH) which crop out to the northeast and an area of Neogene olivine and augite-bearing basalts to the east (Fig. 1). The geology of the Ngorongoro Volcanic Highlands, including Ngorongoro, Lemagaru, Sadiman and the southernmost and closest centre of Oldeani is dominated by basalt, trachyte, phonolite and nephelinite lavas, and pyroclastic rocks of phonolitic, nephelinic and carbonatitic compositions (Dundas et al., 1977; Le Gall et al., 2008; Mollel et al., 2008; Mollel and Swisher, 2012; Zaitsev et al., 2012).

The Luxmanda site lies on the Mbulu Plateau above the northern shore of the seasonal Lake Balangida. At this site the bedrock units, which crop out sporadically in the area, are assigned to the Archean Tanzanian Craton although the site is close to the shear zone contact with the Western Granulites of the Mozambique Belt. This area mostly receives drainage from Archean metamorphic basement rocks of the Mbulu Plateau which are dominantly granitic in composition (Thomas, 1963). Whilst the geophysical characteristics of the Luxmanda archaeological site (Fitton et al., 2022) and the influence of human occupation on the soil chemistry (Storozum et al., 2021) have been described, there are no detailed mineralogical descriptions available either for the local

bedrock geology or the superficial sediment cover in the area.

3. Methodology and samples studied

Thirteen pottery samples, eleven (11) from Luxmanda and two (2) from Mumba Rockshelter were selected for analysis. The sherds were collected from different excavation units and stratigraphic levels to minimise the possibility of sampling fragments from the same vessel (Table 1, Fig. 2). The samples from Mumba Rockshelter were included in this study to test if, given the two sites' relative geographic proximity, ceramics were either being produced with raw materials from the same clay sources or potentially exchanged between them (Ombori, 2021). The samples were prepared as polished petrographic thin sections and examined using polarising light microscopy (Whitbread, 1996; Quinn, 2013, 2022). The thin sections were then carbon coated and the mineralogy / phases present quantified using automated scanning electron microscopy.

Table 1
Summary of pottery samples analysed in this study.

Site	Thin Section	Sample Number	Excavation Unit	Level	Description
Luxmanda	1	1302A	18	3	Pale brown to dark brown body sherd, undecorated
Luxmanda	2	1245	17	9	Pale brown (Light beige/tan) body sherd, undecorated
Luxmanda	3	1453	19	11	Light brown with dark spots body sherd, undecorated
Luxmanda	4	1002	15	3	Very dark brown (blackish) body sherd, undecorated
Luxmanda	5	2036	25	9	Reddish-brown with darker patches body sherd, undecorated
Luxmanda	6	1505	20	5	Reddish-brown with darker patches body sherd, undecorated
Luxmanda	7	1012	15	5	Light brown (tan) with darker spots body sherd, undecorated
Luxmanda	8	1102	16	3	Dark brown with lighter patches rim sherd, decorated
Luxmanda	9	1970	24	13	Light brown with dark spots body sherd, undecorated
Luxmanda	10	2102B	26	3	Reddish-brown with darker patches body sherd, undecorated
Eyasi	11	Z 0.52	19	10D	Dark brown body sherd, undecorated
Eyasi	12	Z 0.56	19	9C	Dark to pale brown rim sherd, decorated
Luxmanda	13	1620	21	9	Reddish-brown body sherd, undecorated

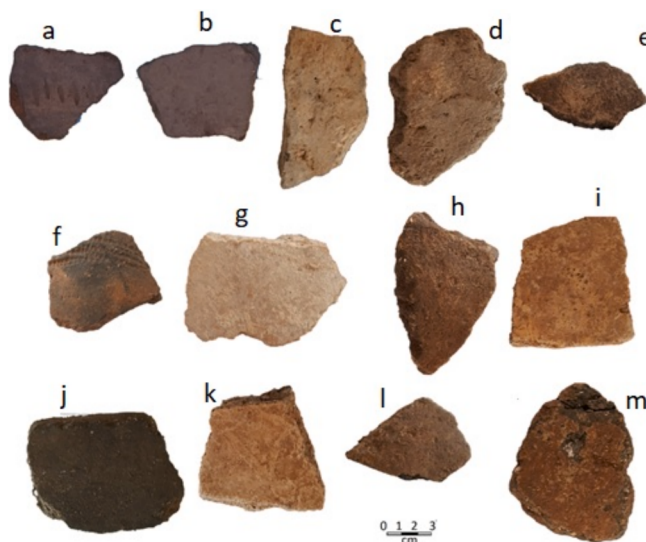


Fig. 2. Ceramic samples selected for mineralogical analysis. Z 0.56 (a), Z 0.52 (b), 1970 (c), 1453 (d), 1620 (e), 1102 (f), 1245 (g), 1505 (h), 2036 (i), 1002 (j), 1012 (k), 1302A (l), 2102B (m). Samples (a) and (b) (Z 0.56 and Z 0.52, respectively) are from Mumba Rockshelter, all of the rest are from Luxmanda. Figure modified from Ombori (2021).

3.1. Optical polarising light microscopy

Pottery samples examined in this study were prepared for thin section microscopy. The samples were first vacuum impregnated with a mixture of five parts Hardrock 554 epoxy resin and one part Hardrock 554 hardener and cut using a diamond saw (Ombori, 2021). An epoxy impregnation process was used to stabilise the samples with a plastic moulding compound to withstand subsequent cutting and polishing. The samples were then fixed to glass slides and abraded until a standard thickness of 30 µm was attained (Whitbread, 1996; Reedy, 1994, 2008; Peterson and Betancourt, 2009; Quinn, 2013, 2022). Thin section slides were later analysed using a Leica DM 750 polarising light microscope equipped with a digital camera following standard procedures. Optical microscopy complements automated mineralogy in that some petrographic textural features cannot be observed using automated mineralogy, while conversely, determining the mineralogy of the clay matrix and its fired equivalents, along with any opaque phases present, cannot be achieved with polarising light microscopy.

3.2. Automated SEM-EDS

Automated SEM-EDS is a widely adopted analytical methodology in the Earth sciences (e.g. Schulz et al., 2020) and has previously been used in archaeological studies of ceramics (e.g. Knappett et al., 2011; Hill-ditch et al., 2012, 2016; Frigóle et al., 2019; Menzies et al., 2015) along with the analysis of archaeological raw materials (e.g. Bevins et al., 2020, 2021, 2022, 2023; Nash et al., 2021) and associated sediments / soils (e.g. Brown et al., 2021, 2022; Ward et al., 2017, 2019, 2022a, 2022b). However, whilst the AMICS platform has been used in previous archaeological studies (e.g. Bevins et al., 2023) it has not been previously widely used in ceramic analysis, hence the analytical parameters are described here. In this study, automated SEM-EDS analysis was undertaken using a Hitachi SU3900 scanning electron microscope fitted with dual large area (60 mm^2) Bruker SDD energy dispersive spectrometers and running the AMICS automated mineralogy package. Beam conditions are optimised for analysis and therefore an accelerating voltage of 20 kV coupled with a beam current of approximately 15 nA were used. The samples were measured using the segmented field image mode of analysis. This analytical mode subdivides the backscatter

electron (BSE) image into domains (segments) of similar brightness which represent different mineral grains / phases and then acquires a representative EDS X-ray spectrum from a point within the segment; the mineral/phase identified is then assigned to the entire segment. Measurements are optimised to highlight both textural and modal mineralogical information and so an effective image resolution of 2 µm was achieved.

The EDS spectra acquired during the measurement are compared with a library of measured and synthetic standards and a mineral identification is made on a closest match basis. Phases which are not represented in the standards list at the time of measurement are added either by acquiring reference spectra directly from the sample, or by creating a reference spectrum from the measurement itself. As the standards list can comprise hundreds of reference spectra, the data are grouped into a final, more manageable, reported mineral list. The mineralogical groupings used in this study are provided in Table 2. Note that whilst data collection is automated, the mineral classification scheme used needs to be adapted for each project (cf. Carloni et al., 2022) although as more examples of a class of material (e.g. ceramics) are analysed then the initial database developed will require less project specific modification. Data outputs from analysis include the area % modal mineralogy, along with compositional maps of the areas analysed along with the corresponding area SEM-BSE images.

The mineralogy data for the analysed samples is presented in Table 3. These data provide the area % mineralogy for the constituent particulate mineral inclusions and the ceramic clay matrix / paste combined. Based

Table 2
Automated mineralogy compositional groups used to process the data.

Mineral group	Description
Quartz	Silica group of minerals (e.g. quartz, cristobalite, etc). Includes opal and chert.
K Feldspar	K-rich alkali feldspar including orthoclase, sanidine & microcline.
Plagioclase	Albite to anorthite solid solution.
Muscovite	Muscovite and Al-rich white mica such as sericite.
Mg Fe K Al silicate	Mg- and Fe-bearing K Al silicate phases such as biotite, phlogopite, fired ceramics.
Kaolinite	Kaolinite and dickite. May also include tourmaline.
Chlorite	Chlorite group minerals such as chamosite and clinochlore etc. May include specific compositions of garnet, cordierite and / or staurolite if present.
Illite	Illite and illite-dominant illite-smectite
Orthoamphibole	Ca-poor amphiboles such as anthophyllite. May include other Mg silicates such as orthopyroxene and talc.
Clinoamphibole	Amphiboles such as hornblende and actinolite. May also include clinopyroxene.
K Fe Al silicate	K and Fe-bearing aluminosilicates. May include fine mixtures of illite and Fe oxides.
Fe silicate	Fe silicates such as fayalite. Also includes fine mixtures of Fe oxides and silica.
Ca Al silicate	Ca silicates such as wollastonite. May also include fine mixtures of calcite and silica.
Al silicate	Al silicates. Typically contains minor quantities of K and Fe.
Mn phases	Mn phases such as Mn oxides, Mn silicates (e.g. spessartine garnet) etc.
Kyanite	Al-rich aluminosilicates such as kyanite, andalusite, and sillimanite.
Epidote	Fe-bearing Ca Al silicate phases. May also include prehnite, zoisite, and chemically similar ceramic phases.
Calcite	Calcite and ferroan calcite.
Dolomite	Dolomite and ferroan dolomite. May include high Mg calcite.
Pyrite	Pyrite and marcasite.
Barite	Barite and celestine.
Fe Oxides	Fe oxides such as magnetite and hematite, Fe hydroxides and siderite.
Ti Oxides	Ti oxides such as anatase and rutile.
Ilmenite	Ilmenite and Ti-rich magnetite.
Titanite	Titanite.
Apatite	Apatite, hydroapatite and francolite.
Zircon	Zircon and hafnon.
Undifferentiated	Any other phases not included above.

Table 3
Automated mineralogy (area %) data.

Samples	1302 A	1245	1453	1002	2036	1505	1012	1102	1970	2102B	Z 0.52	Z 0.56	1620
Porosity	11.4	12.9	21.3	19.4	13.3	15.0	8.6	16.0	14.7	21.7	22.6	22.3	14.8
Quartz	24.96	26.05	20.41	24.68	33.16	30.67	22.83	19.57	17.85	20.99	17.85	16.66	28.63
K Feldspar	9.15	10.01	12.82	10.76	13.85	14.85	9.28	2.63	8.54	10.91	9.89	7.50	13.09
Plagioclase	7.02	5.98	14.59	6.46	6.35	7.50	6.26	14.43	5.73	6.92	18.70	15.20	8.06
Muscovite	0.50	0.30	0.19	0.37	0.36	0.37	0.37	2.55	0.66	1.06	0.33	0.59	0.43
Mg Fe K Al silicate	19.27	16.65	20.32	16.86	12.43	16.57	23.90	13.71	16.63	19.27	18.59	26.47	15.86
Kaolinite	0.38	0.47	0.66	0.74	0.58	0.34	0.51	0.28	0.54	0.60	3.88	1.23	0.58
Chlorite	0.05	0.05	0.32	0.06	0.04	0.06	0.08	2.11	0.07	0.07	0.86	0.91	0.06
Illite	17.23	19.37	8.33	15.01	9.81	11.39	12.78	9.08	10.53	10.04	8.66	12.66	10.26
Ortho-amphibole	0.01	0.01	0.04	0.02	0.02	0.01	0.01	0.94	0.01	0.01	0.22	0.15	0.02
Clino-amphibole	0.07	0.07	0.31	0.07	0.08	0.08	0.08	3.65	0.10	0.12	1.01	1.94	0.09
K Fe Al silicate	7.61	8.08	13.59	8.19	12.67	6.34	9.12	22.23	26.71	18.12	10.83	11.15	9.20
Fe Silicate	0.01	0.02	0.05	0.01	0.01	0.02	0.39	0.01	0.01	0.01	0.03	0.04	0.02
Ca Al silicate	0.03	0.01	0.02	0.02	0.00	0.00	0.01	0.02	0.02	0.02	0.00	0.02	0.00
Al silicate	13.20	12.30	7.77	16.24	9.87	11.22	14.12	5.24	11.45	11.26	8.34	4.02	12.98
Mn Phases	0.04	0.09	0.12	0.07	0.09	0.04	0.08	0.07	0.15	0.03	0.12	0.05	0.16
Kyanite	0.01	0.00	0.00	0.00	0.02	0.01	0.00	0.01	0.06	0.02	0.02	0.06	0.01
Epidote	0.18	0.18	0.03	0.20	0.24	0.22	0.21	0.06	0.23	0.21	0.14	0.07	0.24
Calcite	0.01	0.05	0.01	0.00	0.00	0.00	0.00	0.05	0.00	0.00	0.01	0.71	0.00
Dolomite	0.00	0.00	0.00	0.00	0.00	0.00	0.00	0.00	0.00	0.00	0.00	0.02	0.00
Pyrite	0.00	0.00	0.00	0.00	0.00	0.00	0.00	0.00	0.00	0.01	0.00	0.00	0.00
Barite	0.00	0.00	0.00	0.00	0.01	0.00	0.00	0.01	0.01	0.02	0.00	0.02	0.00
Fe Oxides	0.03	0.03	0.08	0.01	0.02	0.02	0.03	1.49	0.03	0.03	0.06	0.13	0.02
Ti Oxides	0.03	0.05	0.07	0.04	0.05	0.05	0.06	0.03	0.04	0.02	0.08	0.06	0.04
Ilmenite	0.06	0.08	0.06	0.06	0.07	0.12	0.05	0.18	0.06	0.08	0.22	0.15	0.08
Titanite	0.02	0.02	0.02	0.02	0.04	0.02	0.04	0.04	0.03	0.03	0.05	0.04	0.02
Apatite	0.03	0.01	0.07	0.01	0.01	0.02	0.09	1.01	0.02	0.01	0.01	0.06	0.01
Zircon	0.02	0.01	0.03	0.02	0.11	0.03	0.02	0.02	0.39	0.04	0.05	0.02	0.05
Other	0.08	0.09	0.06	0.07	0.10	0.05	0.06	0.23	0.13	0.08	0.04	0.08	0.08

on the automated mineralogy compositional maps the modal data are divided into (a) minerals forming the constituent particulate inclusions and (b) the ceramic clay matrix / paste. The mineral inclusions present may either be monomineralic (composed of a single mineral) or poly-mineralic, representing small lithic (rock) fragments. Within this dataset, any lithic grains present are reported as the constituent minerals rather than the lithic grain types. However, the presence of lithic grains is apparent within the automated mineralogy compositional maps, which provide the mineralogical data in textural context. However, it should be noted that with automated SEM-EDS analysis of granular / particulate materials it is possible to automatically classify poly-mineralic component grains into lithological classes (i.e. rock types) (e.g. Pirrie et al., 2013). However, as discussed by Carloni et al. (2022) this is more difficult with the traditional automated SEM-EDS platforms, although should become possible with the AMICS system through the integration of the automated SEM-EDS compositional map and the SEM backscattered electron image of the corresponding area. Whilst Carloni et al. (2022) argue that mineral identification based on crystallographic properties is a strong advantage of optical microscopy versus the mineral identification based on chemistry via automated SEM-EDS, we would contest that many critical parameters for robust optical mineral identification are commonly not possible to achieve in ceramic thin sections; nor is it possible to identify the mineralogy / composition of the clay matrix or opaque phases. Fundamentally all methods have strengths and weaknesses and the integration of different analytical methods provides the highest resolution data.

4. Results

Based on the combined results of both the polarising light microscopy and the automated SEM-EDS analysis, a number of distinct compositional groups are recognised. Whilst there are broad similarities among all of the analysed samples, based on the petrography, automated SEM-EDS modal mineralogy and the textural images, they are divided into four distinct compositional groups. The 11 samples from Luxmanda can be divided into three compositional groups (A, B and C), whilst the

two samples from Mumba Rockshelter define a distinct fourth compositional Group D (Fig. 3).

4.1. Compositional Group A

Group A is the dominant compositional group including 9 of the analysed samples from Luxmanda (1302A, 1245, 1002, 2036, 1505, 1012, 1620, 1970 and 2102B). Within this compositional group the particulate (mineral) inclusions are dominantly composed of quartz (17.85–33.16 %), K feldspar (8.54–10.91 %) and plagioclase (5.73–7.02 %). Other minerals present in some or all of the samples at an abundance of ~ 1 % or less are: muscovite, orthoamphibole, clinoamphibole, Mn phases, kyanite, epidote, calcite, pyrite, barite, Fe oxides, Ti oxides, ilmenite, titanite, apatite, zircon and “undifferentiated” (Table 3, Fig. 3). The clay paste / matrix is dominantly composed of Mg Fe K Al silicate (16.65–23.90 %), illite (10.04–19.37 %) and Al silicate (11.26–16.24 %) along with less abundant K Fe Al silicate (7.61–26.71 %) and at an abundance of ~ 1 % or less, Fe silicate, Ca Al silicate, kaolinite and chlorite. Texturally, this compositional group has abundant matrix/clay paste, along with mineral inclusions of sand-grade disseminated quartz, K feldspar and plagioclase. These grains are typically subangular in shape. The matrix / ceramic paste has a strongly defined fabric, with abundant porosity, typically developed parallel with the foliation in the ceramic paste. The automated mineralogy data for this compositional group are shown in Fig. 3, where the mineral groups forming the inclusions are plotted separately to the mineral phases which will be present predominantly within the clay matrix / paste. Typically, approximately 40–55 % of the area is composed of inclusions with 45 to 65 % clay paste. Whilst there is some variance in the relative abundance of inclusions to clay paste, the samples within this group are compositionally very similar.

The polarising light microscopy results show that the inclusions in these samples are dominated by both monocrystalline and polycrystalline quartz. The quartz grains typically show undulose extinction. Feldspars are also abundant and include grains of plagioclase and K feldspar, with abundant microcline (Fig. 4) and less common perthitic

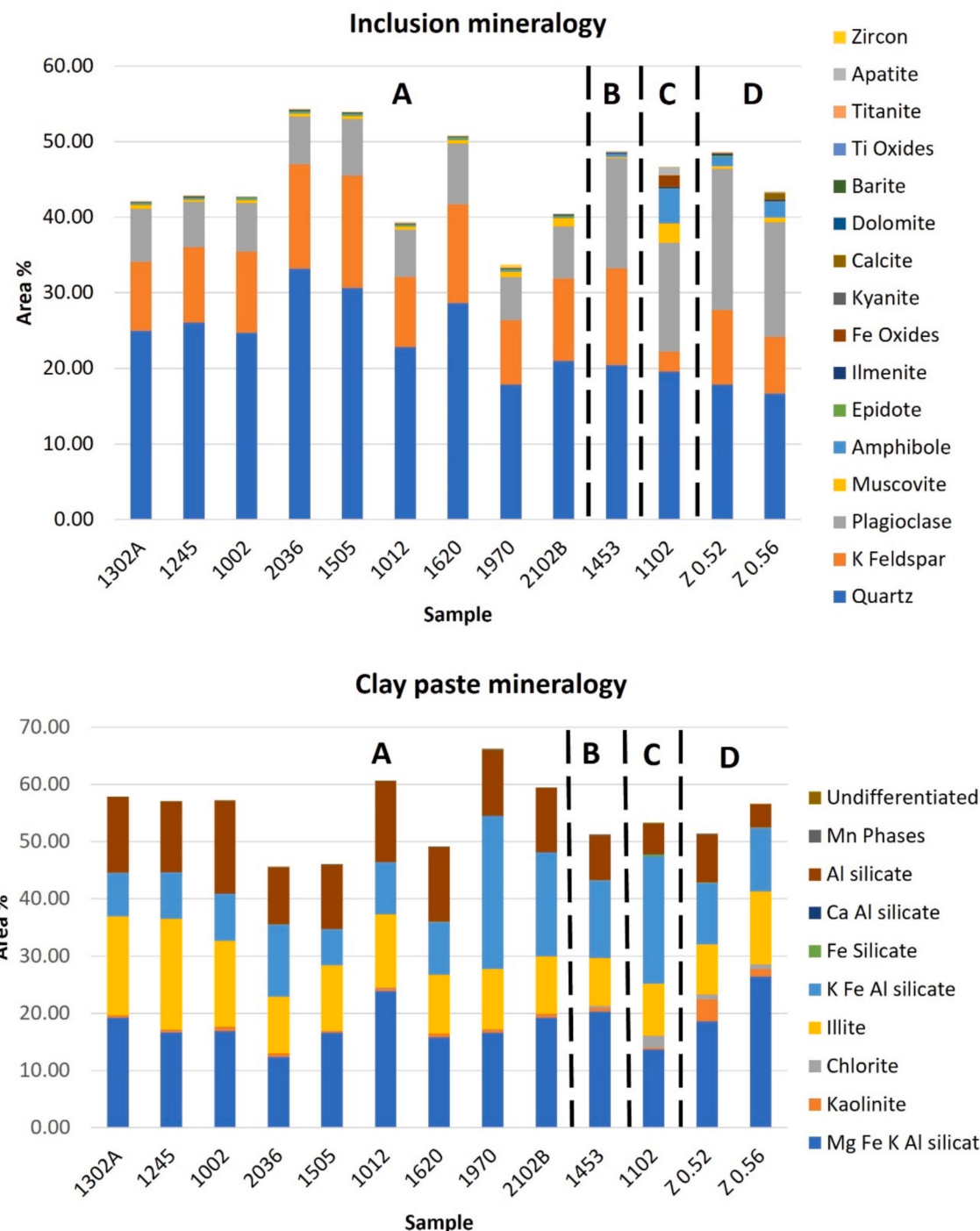


Fig. 3. Automated SEM-EDS modal mineralogy data for both the inclusions and the clay pastes, allowing the definition of four compositional groups A, B, C and D (see text for detail).

feldspar grains. Lithic rock fragments are present as inclusions and are composed of quartz and feldspar with evidence for ductile deformation fabrics. Rare grains of amphibole, possibly tourmaline and calcite also occur as do very rare inclusions of charcoal (Fig. 4). The modal mineralogy and petrography for compositional Group A indicates that the aggregate grains used in pottery manufacture were derived from a granitic / granitic gneiss source terrane.

4.2. Compositional Group B

Compositional Group B is defined on the basis of a single sample

(Sample 1453). The particulate mineral inclusions in this sample are dominated by quartz (20.41 %), K feldspar (12.82 %) and plagioclase (14.59 %). Other minerals present at an abundance of ~ 1 % or less are: muscovite, amphibole, epidote, ilmenite, Fe oxides, calcite, Ti oxides, titanite, apatite, zircon, Mn phases and undifferentiated (Table 3, Fig. 3). The clay paste / matrix is composed of Mg Fe K Al silicate (20.32 %) and K Fe Al silicate (13.59 %), along with less abundant illite (8.33 %) and Al silicate (7.77 %) and, at an abundance of ~ 1 % or less, kaolinite, chlorite, Fe silicate and Ca Al silicate. In comparison with compositional Group A, the key differences are the significantly increased abundance of plagioclase and decreased abundance of quartz,

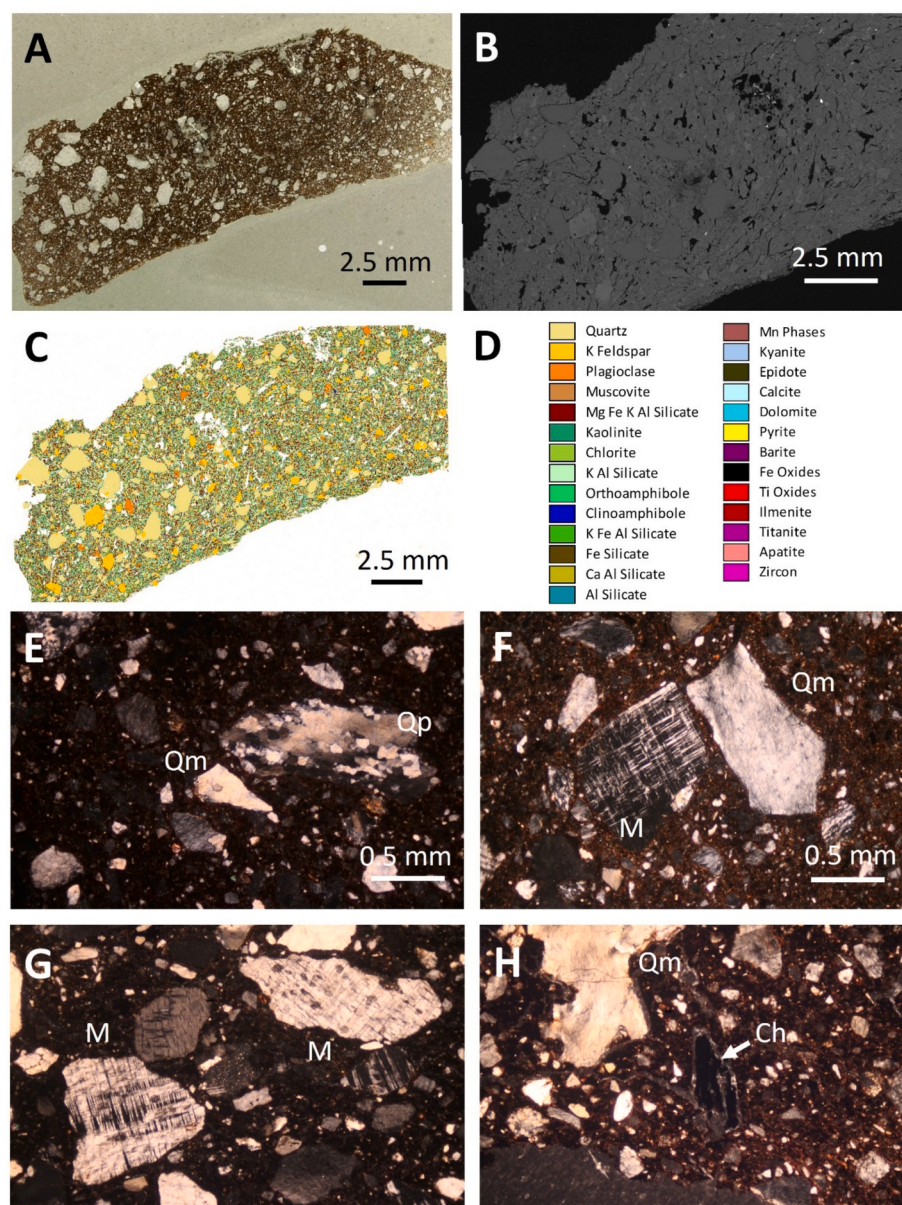


Fig. 4. Petrography of pottery compositional Group A (A, B, C, E, F Sample 1302A; G Sample 1505; H Sample 2102B). (A) Representative binocular microscope image of pottery fabric. (B) SEM backscatter electron image; dark areas highlight the porosity. (C, D) Automated SEM-EDS false colour image and key. (E) Cross polarised light thin section photomicrograph; note polycrystalline (Qp) and monocrystalline (Qm) quartz grains. (F) Cross polarised light thin section photomicrograph; note large angular microcline (M) grains and monocrystalline quartz showing undulose extinction. (G) Cross polarised light thin section photomicrograph; note large angular microcline (M) grains. (H) Cross polarised light thin section photomicrograph; note monocrystalline (Qm) quartz and presence of charcoal (Ch) fragment (arrowed).

illite and Al silicate. The automated mineralogy data for compositional Group B are shown in Fig. 3, where the mineral groups forming the mineral inclusions are plotted separately to the mineral phases which are present predominantly within the clay matrix / paste.

In thin section, the inclusions in compositional Group B comprise abundant undulose extinction monocrystalline and less commonly polycrystalline quartz. Feldspar is abundant and includes plagioclase, K feldspar, abundant microcline and perthitic feldspars (Fig. 5). Rock fragments are absent from this sample, although this could be a function of the grain size of the particulate inclusions and / or the original source lithology. Rare tourmaline and amphibole is present as are Fe oxides. The characteristic features allowing Group B to be separated from Group A are the significantly increased abundance of plagioclase and decreased abundance of quartz, illite and Al silicate along with the apparent absence of rock fragments. The ratio of K feldspar to plagioclase in this

compositional group is 0.88, which differs to compositional Group A which has an average ratio of 1.66. Whilst a similar provenance for the mineral grains used in pottery manufacture is indicated with at least in part, derivation from a granitic / granitic gneiss source terrane, the increased abundance of plagioclase relative to K feldspar may indicate a different, or mixed, provenance.

4.3. Compositional Group C

Compositional Group C also comprises one sample (1102) from Luxmunda. In this sample the particulate mineral inclusions are dominated by quartz (19.57 %) and plagioclase (14.43 %) along with less abundant K feldspar (2.63 %), muscovite (2.55 %), amphibole (4.59 %), Fe oxides (1.49 %) and apatite (1.01 %). Other minerals present at an abundance of ~1 % or less are: epidote, ilmenite, kyanite, calcite, barite,

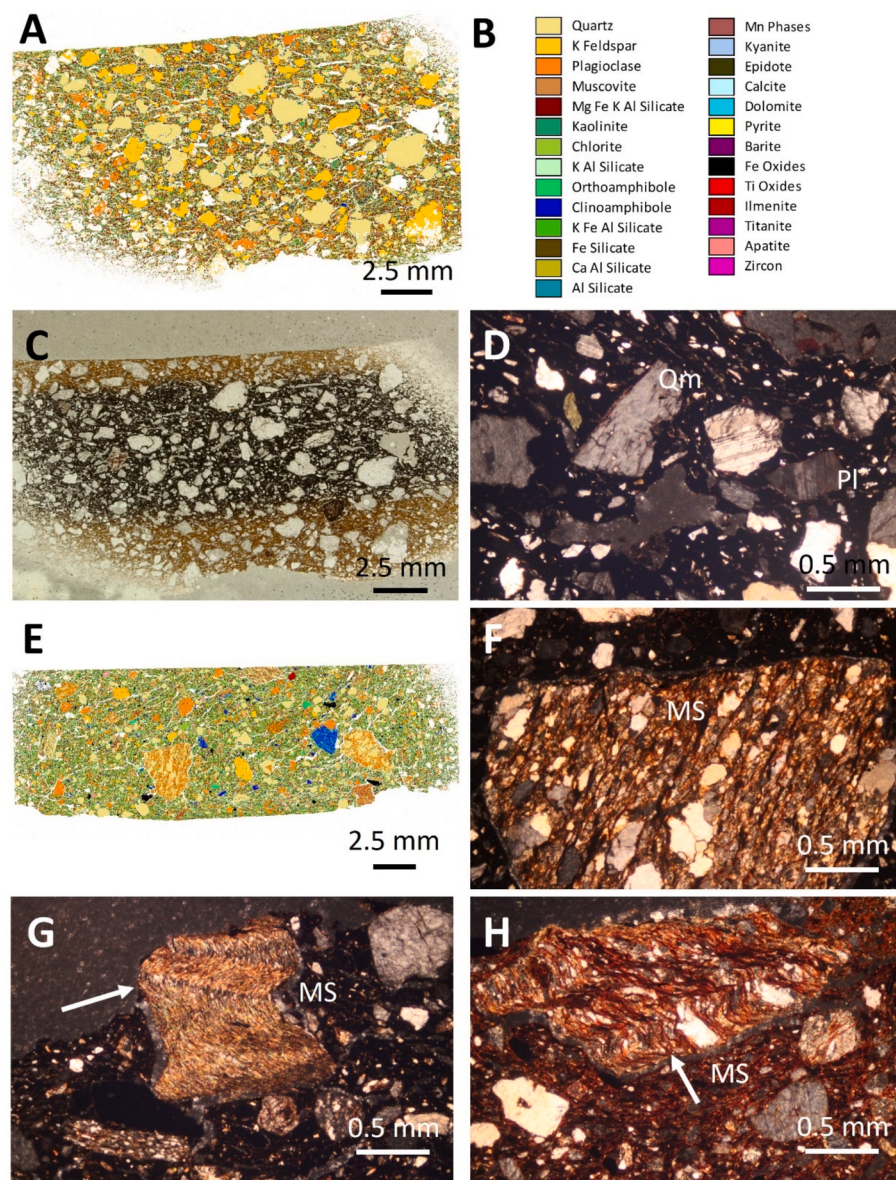


Fig. 5. Petrography of pottery compositional groups B and C. A, C, D – compositional Group B, Sample 1453. E, F, G, H – compositional Group C, Sample 1102. (A, B) Automated SEM-EDS false colour image and key, compositional group B. (C) Binocular microscope image of pottery fabric. (D) Cross polarised light thin section photomicrograph; note monocrystalline (Qm) quartz and plagioclase (Pl) feldspar. (E) Automated SEM-EDS false colour image compositional group B; key as in (B). (F) Cross polarised light thin section photomicrograph; note large metasedimentary rock fragment (MS). (G) Cross polarised light thin section photomicrograph; note presence of metasedimentary (MS) rock fragment (arrowed) with refolded cleavage, implying derived from a polyphase deformed terrane. (H) Cross polarised light thin section photomicrograph; note presence of metasedimentary (MS) rock fragment with refolded cleavage (arrowed), implying derivation from a polyphase deformed terrane.

Ti oxides, titanite, zircon, Mn phases and undifferentiated (Table 3, Fig. 3). The clay paste / matrix is composed of dominant K Fe Al silicate (22.23 %) and Mg Fe K Al silicate (13.71 %) along with less abundant chlorite (2.11 %), illite (9.08 %) and Al silicate (5.24 %). Other minerals present at an abundance of ~1 % or less are: kaolinite, Fe silicate and Ca Al silicate. In comparison with compositional Group A, the key characteristics of Group C are the significantly increased abundance of plagioclase, muscovite, amphibole, Fe oxide, apatite and chlorite and decreased abundance of epidote, illite and Al silicate.

In thin section, Sample 1102 which forms compositional Group C is distinctive in that the particulate mineral inclusions are composed of abundant metasedimentary rock fragments (Fig. 5). The metasedimentary rock fragments are dominantly composed of pelites and psammite grains, commonly displaying a well-developed cleavage and / or microfolding (Fig. 5). Some lithic grains show partial alteration to

carbonate. Rare grains interpreted as derived from cataclasites are also present. Other grains include undulose extinction monocrystalline and polycrystalline quartz, plagioclase, K feldspar, microcline and perthite. The overall mineralogical and petrological characteristics for Group C suggest that the sand-grade mineral inclusions were derived from a metasedimentary (pelite-psammite) source terrane which has undergone polyphase deformation as evidenced by the refolded cleavage evident in some of the grains.

4.4. Compositional Group D

Compositional Group D is composed of the two samples from Mumba Rockshelter (samples Z 0.52 and Z 0.56). The particulate mineral inclusions in this compositional group sample are dominated by quartz (16.66–17.85 %) and plagioclase (15.20–18.70 %) along with less

abundant K feldspar (7.50–9.89 %) and amphibole (1.23–2.08 %). Other minerals present at an abundance of ~ 1 % or less are: muscovite, epidote, ilmenite, Fe oxides, kyanite, calcite, dolomite, barite, Ti oxides, titanite, apatite, zircon, chlorite, Fe silicate, Ca Al silicate, Mn phases and undifferentiated (Table 3, Fig. 3). The clay paste / matrix is composed of dominant Mg Fe K Al silicate (18.59–26.47 %), K Fe Al silicate (10.83–11.15 %) and illite (8.66–12.66 %) along with less abundant kaolinite (1.23–3.88 %) and Al silicate (4.02–8.34 %) and chlorite, Fe silicate and Ca Al silicate, at an abundance of ~ 1 % or less.

Petrographically the mineral inclusions within the two samples making up Group D are dominated by monocrystalline and polycrystalline quartz showing undulose extinction and plagioclase with less abundant K feldspar and microcline (Fig. 6). Amphibole is abundant along with muscovite and possible tourmaline. Lithic grains are rare. In comparison with compositional Group A, Group D comprises significantly less K feldspar and Al silicate and more abundant plagioclase, amphibole, ilmenite, kaolinite and chlorite. Whilst in compositional Group A the ratio of K feldspar to plagioclase ranges between 1.30 and

2.18 (average 1.66), so that K feldspar is always more abundant than plagioclase, within compositional Group D this differs, so that plagioclase is greater than K feldspar at a ratio of 0.49 and 0.53. Overall, the mineralogy of Group D is broadly consistent with raw materials being sourced from granitic gneisses.

5. Interpretation

Automated SEM-EDS characterisation of Narosura pottery from Luxmanda provides useful insights into the raw material sourcing strategies of an ancient eastern African PN community. All three compositional groups are consistent with the raw materials being derived from source areas associated with the Precambrian basement rocks, rather than either the rift-related sedimentary rocks or volcanic units. The same is true of the compositional group identified for samples from Mumba Rockshelter. Present day pottery production on the Mbulu Plateau is focussed around villages to the NE of Luxmanda, in an area underlain by Precambrian basement rocks, with locally sourced raw materials

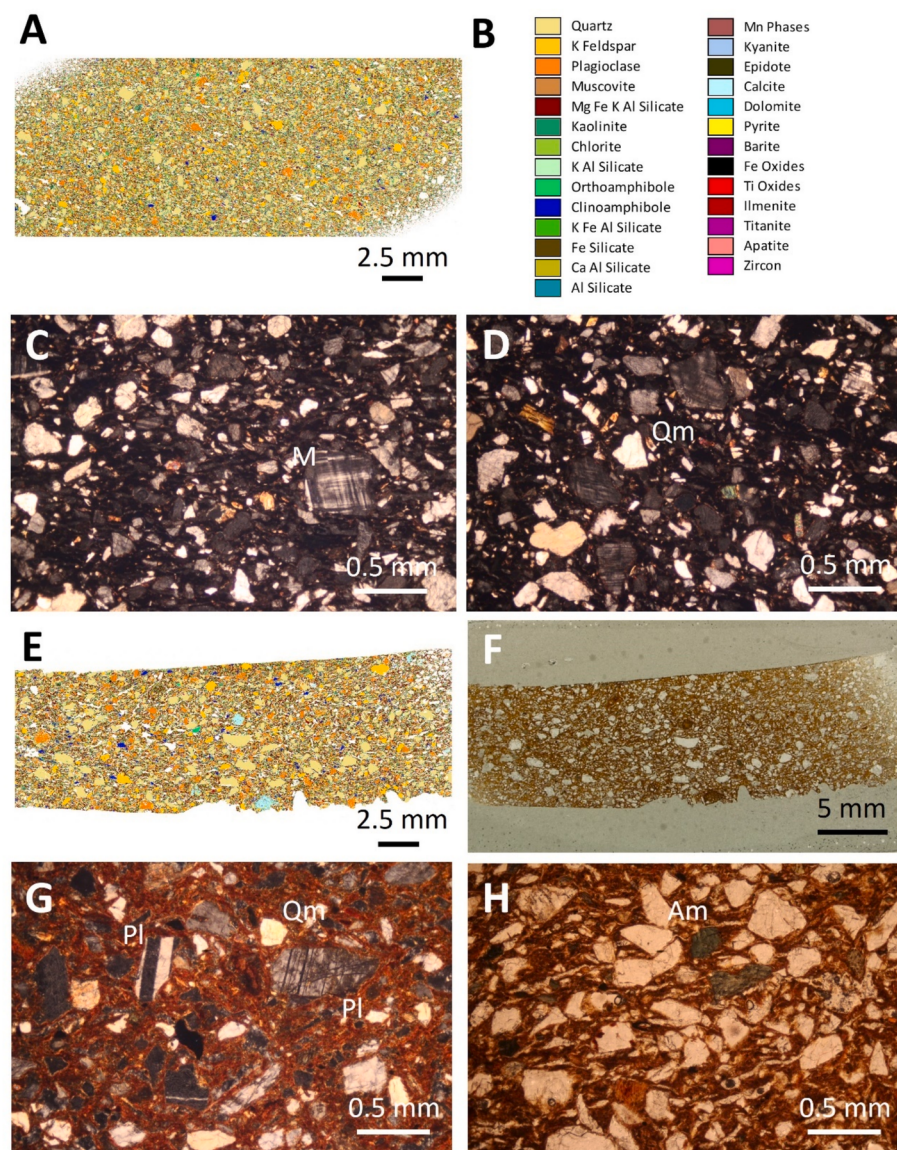


Fig. 6. Petrography of pottery compositional Group D. A, C, D – Sample Z 0.52. E, F, G, H – Sample Z 0.56. (A, B) Automated SEM-EDS false colour image and key, compositional group D, Sample Z 0.52. (C) Cross polarised light thin section photomicrograph; note microcline (M) feldspar. (D) Cross polarised light thin section photomicrograph; note monocristalline (Qm) quartz. (E) Automated SEM-EDS false colour image compositional Group D; key as in (B), Sample Z 0.56. (F) Binocular microscope image of pottery Sample Z 0.56. (G) Cross polarised light thin section photomicrograph; note presence of abundant plagioclase (Pl) feldspar and monocristalline (Qm) quartz. (H) Plane polarised light thin section photomicrograph; note presence of abundant amphibole (Am).

(Ombori, 2021). The results reveal several different compositional groups that represent local variations in the raw materials used for pottery production and offer a greater understanding of PN cultural practices. At Luxmanda, the majority of the analysed pottery samples all fall within compositional Group A, with the particulate mineral inclusions interpreted as derived from a granitic or granitic gneiss source area. Both of the major Precambrian bedrock units (the Tanzanian Craton) and the Western Granulites of the Mozambique Belt include granites and granitic gneisses, hence differentiating these two possible sources areas based on the available data is difficult. Thomas (1963) noted that the superficial deposits in the area are dominated by “sandy soils derived from granitic rocks”. Mineral phases making up the fired clay matrix / pastes in the ceramic samples in this compositional group are also a coherent grouping which whilst dominated by Mg Fe K Al silicates and illite also has relatively abundant Al silicates (with a ratio of Mg Fe K Al silicates to Al silicates varying between 1.04 and 1.71) when compared against compositional groups B to D, implying that both the clay paste and also the mineral inclusions were derived from the same source areas.

However, whilst compositional Group A dominates the analysed samples from Luxmanda, two ceramic samples differ both from Group A and each other, and define compositional groups B and C; neither of these is in a unit or level that is archaeologically distinct from the contexts of samples belonging to Group A. These samples show that ceramics, with markedly different clay and sand raw material sources, are also present within the same archaeological context. Whilst compositional Group B is consistent with a granitic or granitic gneiss source, this is clearly distinct to that for compositional Group A; overall the characteristics of this sample may support provenance from a granitic source rock, potentially either the Tanzanian Craton or the Mozambique Belt. Group C is distinctive in that the sand grade grains present are dominated by metasedimentary rock fragments composed of pelites and psammites, commonly displaying a well-developed cleavage and / or microfolding; a source within units assigned to the Mozambique Belt is most likely, although derivation from the Tanzanian Craton is also possible. As compositional groups B and C can clearly be differentiated from Group A, there is no evidence that the initial raw materials, sourced from different locations, were being blended and mixed ahead of ceramic production. However, whether raw materials were transported from farther afield and fired locally at Luxmanda, or whether pottery was derived from other sites of ceramic production and then transported to, and used at, Luxmanda is unknown.

The pottery samples from Mumba Rockshelter (Group D) differ in terms of mineral composition from those of Luxmanda. The samples typically lack lithic grains and are dominated by grains of quartz, plagioclase, K feldspar and amphibole, whilst the clay matrix / paste is dominated by abundant Mg Fe K Al silicates, illite and K Fe Al silicates along with more abundant kaolinite than observed in the other analysed samples. Overall, the mineral assemblage is broadly consistent with raw materials being sourced from granitic gneisses which crop out to the south of Mumba Rockshelter (in the direction of several open-air pastoralist sites with Narosura ware), and source alluvial sediments transported northwards towards Lake Eyasi, and derived from the Tanzanian Craton. The results support relatively locally sourced raw materials with potentially also local sites of ceramic production.

The differences in mineralogical compositions between these two sites and the four identified compositional groups suggest regional variations in raw material sourcing strategies and technological practices, where potters in each community primarily produced pottery from local geological sources. At Luxmanda, potters may have obtained clays from multiple (relatively) local sources. Alternately, some pots produced elsewhere, from clays different than those used by Luxmanda potters, may have been brought to the site. There is no evidence in the samples analysed for raw materials being derived from the geologically much younger rift-related sedimentary or volcanic rocks.

6. Conclusions

This study provides a comprehensive mineralogical characterisation of Narosura pottery from the Luxmanda site, and additional pottery samples from Mumba Rockshelter, in northern Tanzania using automated scanning electron microscopy coupled with energy dispersive spectrometry (SEM-EDS). This analytical approach allows for high-resolution, quantitative assessment of ceramic mineralogy, offering a detailed understanding of the clay matrices, non-plastic inclusions, and ceramic textures. The integration of automated SEM-EDS with optical microscopy has yielded new insights into the raw material sourcing strategies of potters at Luxmanda in the eastern African PN.

This initial study of 13 ceramic samples reveals the use of diverse raw material sources, with the recognition of four discrete compositional groups; three from Luxmanda and a separate group for samples from Mumba Rockshelter. These groups each reflect different geological provenances for the raw materials used during ceramic production, and potentially support localised sites of ceramic production. In the ceramic samples from Luxmanda, the interpreted raw material source areas comprise granite/granitic gneisses (Group A), granitic rocks (Group B) and pelite-psammite metasediments (Group C). Mumba Rockshelter pottery samples (Group D) also displayed a different mineralogical profile interpreted as sediment supply from granitic gneisses, but with a different mineralogical profile, and therefore a different source area, to those from Luxmanda.

The compositional differences between the Luxmanda and Mumba Rockshelter pottery samples suggest regional variations in pottery production and cultural practices. These distinct mineralogical profiles indicate different raw material sourcing strategies, influenced by local geological availability and possibly also cultural preferences. Alternatively, our results may indicate that potters utilizing different sources exchanged finished products through networks that will only be delineated through additional research on both clay sources and archaeological pottery from multiple sites in the region. More detailed raw material provenance determination is limited by the lack of detailed mineralogical data for the main bedrock units and superficial cover units in the area. Further work to characterise the mineralogy of currently exploited raw materials for ceramic production in the region may aid the interpretation. In addition, dating detrital zircon grains could distinguish between the different Precambrian basement units.

CRediT authorship contribution statement

Titus Luomba Ombori: Writing – review & editing, Writing – original draft, Visualization, Resources, Project administration, Methodology, Investigation, Funding acquisition, Formal analysis, Data curation, Conceptualization. **Duncan Pirrie:** Writing – review & editing, Writing – original draft, Software, Methodology, Funding acquisition, Formal analysis, Conceptualization. **Matthew R. Power:** Formal analysis. **Ian Skilling:** Formal analysis. **Agness O. Gidna:** Investigation, Resources, Writing – review & editing. **Audax Z.P. Mabulla:** Investigation, Resources, Writing – review & editing. **Pastory M. Bushozi :** Investigation, Resources, Writing – review & editing. **Mary E. Prendergast:** Writing – review & editing, Funding acquisition, Conceptualization. **Katherine M. Grillo:** Writing – review & editing, Funding acquisition, Conceptualization.

Funding

Sample collection at Luxmanda was funded by a Wenner-Gren Foundation grant to KMG (Gr. 9642) and a National Geographic Society Committee for Research and Exploration grant (NGS-196R-18) to MEP. Sample collection at Mumba was funded by the Volkswagen Stiftung through grant number 881015 & 92047 to PMB. The University of Ferrara is thanked for the funding support received under the Erasmus Mundus joint Doctorate Degree from the EACEA Commission of the

European Union which supported the doctoral studies by Titus Ombori.

Acknowledgements

Permission to conduct research at and export samples from Luxmunda and Mumba in 2018 and 2019 was granted to MEP, KMG, and PGM by the Tanzanian Commission on Science and Technology, Ministry of Natural Resources and Tourism (Division of Antiquities), and Ministry of Mines. Fleur Campbell is thanked for draughting figure 1.

Data availability

All data used in this study are presented within the article.

References

- Ambrose, S.H. 1984. The Introduction of Pastoral Adaptations to the Highlands of East Africa. In From Hunters to Farmers: The Causes and Consequences of Food Production in Africa, edited by J. Desmond Clark and Steven Brandt, 212–39. Berkeley, University of California Press.
- Apén, F.E., Rudnick, R.L., Cottle, J.M., Kylander-Clark, A.R.C., Blondes, M.S., Piccoli, P. M., Seward, G., 2020. Four-dimensional thermal evolution of the East African Orogen: accessory phase petrochronology of crustal profiles through the Tanzanian Craton and Mozambique Belt, northeastern Tanzania. *Contrib. Miner. Petrol.* 175, 97.
- Ashley, C.Z., Grillo, K.M., 2015. Archaeological ceramics from Eastern Africa: past approaches and future directions. *Azania: Archaeol. Res. Afr.* 50 (4), 460–480. <https://doi.org/10.1080/0067270X.2015.1102939>.
- Bader, G.D., Bushozi, P., Will, M., Schmid, V., Val, A., Blessing, M., Schmidt, P., Conard, N.J., 2020. Investigating the 1930s Kohl-Larsen collection from the Lake Eyasi Basin, Tanzania. *Mitteilungen Der Gesellschaft Für Urgeschichte* 29, 93–103.
- Bevins, R.E., Pirrie, D., Ixer, R.A., O'Brien, H., Parker Pearson, M., Power, M.R., Shail, R. K., 2020. Constraining the provenance of the Stonehenge ‘Altar Stone’: evidence from automated mineralogy and U-Pb zircon age dating. *J. Archaeol. Sci.* 120. <https://doi.org/10.1016/j.jas.2020.105188>.
- Bevins, R.E., Ixer, R.A., Pirrie, D., Power, M.R., Cotterell, T., Tindle, A., 2021. Alteration fabrics and mineralogy as provenance indicators; the Stonehenge dolerite Bluestones and their enigmatic “spots”. *J. Archaeol. Sci. Rep.* 36, 102826.
- Bevins, R.E., Pearce, N.J.G., Ixer, R.A., Hillier, S., Pirrie, D., Turner, P., 2022. Linking derived debitage to the Stonehenge Altar Stone using portable X-ray fluorescence analysis. *Mineral. Mag.* 1–13. <https://doi.org/10.1180/mgm.2022.22>.
- Bevins, R.A., Pearce, N.J.G., Pirrie, D., Ixer, R.A., Hillier, S., Turner, P., 2023. Assessing the authenticity of a sample taken from the Altar Stone at Stonehenge in 1844 using portable XRD and automated SEM-EDS. *J. Archaeol. Sci. Rep.* 49, 103973.
- Bower, J., 1991. The Pastoral Neolithic of East Africa. *J. World Prehist.* 5, 49–82.
- Brown, A.G., Van Hardenbroek, M., Fonville, T., Davies, K., Mackay, H., Murray, E., Head, K., Barratt, P., McCormick, F., Ficetola, G.F., Henderson, A.C.G., Crone, A., Cavers, G., Langdon, P.G., Whitehouse, N.J., Alsolos, I.G., Pirrie, D., 2021. Ancient DNA, lipid biomarkers and palaeoecological evidence reveals construction and life on early medieval lake settlements. *Sci. Rep.* 11, 11807.
- Brown, A.G., Fonville, T., Van Hardenbroek, M., Cavers, G., Crone, A., McCormick, F., Murray, E., Mackay, H., Whitehouse, N.J., Henderson, A.C.G., Barratt, P., Davies, K., Head, K., Alsolos, I.G., Pirrie, D., 2022. New integrated molecular approaches for understanding lake settlements in NW Europe. *Antiquity*, 2022 page 1 of 21 [10.15184/ajq.2022.70](https://doi.org/10.15184/ajq.2022.70).
- Bushozi, P.G.M. 2023. Mumba rock-shelter, Tanzania. In Beyin, A., Wright, D.K., Wilkins, J., Abdeljalil Bouzouggar, A., Olszewski D.I. (eds), *Handbook of Pleistocene Archaeology of Africa*, 1117–1131. https://doi.org/10.1007/978-3-031-20290-2_73.
- Bushozi, P.M., 2020. Middle and later stone age symbolism: stone beads from Mumba rock-shelter in northern Tanzania. *Utafiti* 15 (1), 1–27.
- Bushozi, P.M., Skinner, A., de Luque, L., 2020. The Middle Stone Age (MSA) technological patterns, innovations, and behavioral changes at bed VIA of Mumba Rockshelter, Northern Tanzania. *African Archaeol. Rev.* 37 (2), 293–310.
- Bushozi, P.M., 2022. Sustainable management and conservation of heritage assets: a case study of the Lake Eyasi Basin, Northern Tanzania. *African Archaeol. Rev.* 39 (3), 303–314.
- Carloni, D., Šegvić, B., Sartori, M., Zanoni, G., Moscariello, A., Besse, M., 2021. Raw material choices and material characterization of the 3rd and 2nd millennium BC pottery from the Petit-Chasseur necropolis: Insights into the megalith-erecting society of the Upper Rhône Valley, Switzerland. *Geoarchaeology* 36, 1009–1044.
- Carloni, D., Šegvić, B., Zanoni, G., Sartori, M., Besse, M., 2022. A critical account of the automated SEM-EDS usage in ceramic analyses at the example of Prehistoric pottery from the site of Petit-Chasseur (3100–1600 BC), southwestern Switzerland. *Mediterr. Archaeol.* 22, 237–259.
- Chami, F., Kwekason, A., 2003. Neolithic pottery traditions from the islands, the coast and the interior of East Africa. *Afr. Archaeol. Rev.* 20, 65–80.
- Collett, D., Robertshaw, P., 1983. Pottery traditions of early pastoral communities in Kenya. *Azania* 18, 107–125.
- Derenne, E., Ard, V., Besse, M., 2020. Pottery technology as a revealer of cultural and symbolic shifts: Funerary and ritual practices in the Sion ‘Petit-Chasseur’ megalithic necropolis (3100–1600 BC, Western Switzerland). *J. Anthropol. Archaeol.* 58, 101170.
- Dundas, D.L., Lloyd Lawrence, A.H., DeQuadros, M., 1977. Lake Eyasi Quarter Degree Sheet 68. Geological Survey of Tanzania.
- Ebinger, C., Djomani, Y.P., Mbude, E., Foster, A., Dawson, J.B., 1997. Rifting Archaean lithosphere: the Eyasi-Manyara-Natron rifts, East Africa. *J. Geol. Soc. Lond.* 154, 947–960.
- Fitton, T., Contreras, D.A., Gidna, A.O., Mabulla, A.Z.P., Prendergast, M.E., Grillo, K.M., 2022. Detecting and mapping the ‘ephemeral’: magnetometric survey of a Pastoral Neolithic settlement at Luxmunda, Tanzania. *Antiquity* 96, 298–318.
- Fletcher, A.W., Abdelsalam, M.G., Emishaw, L., Atekwania, E., Lao-Davila, D., Ismail, A., 2018. Lithospheric controls on the rifting of the Tanzanian Craton at the Eyasi Basin, Eastern Branch of the East African Rift System. *Tectonics* 37, 2818–2832.
- Foster, A., Ebinger, C., Mbude, E., Rex, D., 1997. Tectonic development of the Northern Tanzanian sector of the East African Rift System. *J. Geol. Soc. Lond.* 154, 689–700.
- Frígole, C., Riera-Soto, C., Menzies, A., Barraza, M., Benítez, A., Winocur, D., 2019. Estudio de pastas cerámicas del centro-oeste Argentino (Mendoza, Argentina): microscopía óptica y QEMSCAN. *Boletín De Arqueología PUCP* 27, 67–85.
- Glascock, M.D., Neff, H., 2003. Neutron activation analysis and provenance research in archaeology. *Meas. Sci. Technol.* 14 (9), 1516.
- Gifford, D., Isaac, G., Nelson, C.M., 1980. Evidence for predation and pastoralism at Prolonged Drift: a pastoral Neolithic site in Kenya. *Azania* 15, 57–108.
- Gifford-Gonzalez, D., 1998. Early Pastoralists in East Africa: Ecological and social dimensions. *J. Anthropol. Archaeol.* 17, 166–200.
- Gliganic, I.A., Jacobs, Z., Roberts, R.G., Domínguez-Rodrigo, M., Mabulla, A.Z., 2012a. New ages for Middle and later Stone Age deposits at Mumba rock shelter, Tanzania: optically stimulated luminescence dating of quartz and feldspar grains. *J. Hum. Evol.* 62 (4), 533–547.
- Gliganic, I.A., Jacobs, Z., Roberts, R.G., 2012b. Luminescence characteristics and dose distributions for quartz and feldspar grains from Mumba rockshelter, Tanzania. *Archaeol. Anthropol. Sci.* 4, 115–135.
- Goldstein, S., 2018. The lithic assemblage from Suganya, a Pastoral Neolithic Site of the Elmenteitan tradition in Southwestern Kenya. *Azania: Archaeol. Res. Afr.* 1–29. <https://doi.org/10.1080/0067270X.2018.1540216>.
- Grillo, K.M., Prendergast, M.E., Contreras, D.A., Fitton, T., Gidna, A.O., Goldstein, S.T., Knisley, M.C., Langley, M.C., Mabulla, A.Z., 2018. Pastoral Neolithic settlement at Luxmunda, Tanzania. *J. Field Archaeol.* 43 (2), 102–120.
- Grillo, K.M., Dunne, J., Marshall, F., Prendergast, M.E., Casanova, E., Gidna, A.O., Janzen, A., Karega-Munene, Keute, J., Mabulla, A.Z., Robertshaw, P., Gillard, T., Walton-Doyle, C., Whelton, H.L., Ryan, K., Evershed, R.P., 2020. Molecular and isotopic evidence for milk, meat, and plants in prehistoric eastern African herder food systems. *Proc. Natl. Acad. Sci.* 117(18), 9793–9799.
- Grillo, K.M., Mc Keeby, Z., Hildebrand, E.A., 2022. ‘Nderit Ware’ and the Origins of Pastoralist Pottery in Eastern Africa. *Quat. Int.* 608–609, 226–242. <https://doi.org/10.1016/j.quaint.2020.06.032>.
- Hilditch, J., Knappett, C.J., Pirrie, D., Power, M., 2012. Iasos pottery fabrics and technologies. In: Momigliano, N. (ed) *Bronze Age Carian Iasos, structures and finds from the Roman Agora*. Archeologica 166, Missione Archeologica Italiana Di Iasos, 58–106.
- Hilditch, J., Pirrie, D., Knappett, C., Rollinson, G.K., Momigliano, N., 2016. Taking the rough with the smooth: using automated SEM-EDS to integrate coarse and fine ceramic assemblages in the Bronze Age Aegean. In: Sibbesson, E., Jervis, B. & Coxon, S. (eds), *Insights from innovation: new light on archaeological ceramics*, Highfield Press, 74–96.
- Janzen, A., Balasse, M., Ambrose, S.H., 2020. Early Pastoral Mobility and Seasonality in Kenya Assessed through Stable Isotope Analysis. *J. Archaeol. Sci.* 117, 105099. <https://doi.org/10.1016/j.jas.2020.105099>.
- Kelly, A., Freely, M., Lynch, E.P., Rollinson, G.K., 2014. An imported flanged rimsherd discovered on the early medieval site of Kilree 3, Ireland: a study in archaeological deposition and provenance using automated SEM-EDS analysis (QEMSCAN). *Ceram. Atlantic Connections* 25–38.
- Klehm, C.E., Helper, M.A., Hildebrand, E., Ndiema, E., Grillo, K.M., 2023. Mineralogy and sourcing of a stone bead industry found in communal cemeteries associated with Eastern Africa’s first Pastoralists, ca. 5000 b.p. *J. Field Archaeol.* 1–20. <https://doi.org/10.1080/00934690.2023.2232703>.
- Knappett, C., Pirrie, D., Power, M.R., Nikolakopoulou, I., Hilditch, J., Rollinson, G.K., 2011. Mineralogical analysis and provenancing of ancient ceramics using automated SEM-EDS analysis (QEMSCAN®): a pilot study on LB I pottery from Akrotiri, Thera. *J. Archaeol. Sci.* 38, 219–232. <https://doi.org/10.1016/j.jas.2010.08.022>.
- Kohl-Larsen, L., 1943. Auf den Spuren des Vormenschen, 2 vols., Stuttgart: Strecker und Schröder Verlag.
- Langdon, J., Robertshaw, P., 1985. Petrographic and physico-chemical studies of early pottery from South-Western Kenya. *Azania* 20, 1–28.
- Le Gall, B., Nonnotte, P., Rolet, J., Benoit, M., Guillou, H., Mousseau-Nonnotte, M., Albaric, J., Deverchère, J., 2008. Rift propagation at craton margin. Distribution of faulting and volcanism in the North Tanzanian Divergence (East Africa) during Neogene times. *Tectonophysics* 448, 1–19.
- Marshall, F., 1990. Origins of specialized pastoral production in East Africa. *Am. Anthropol.* 92 (4), 873–894.
- Mehlman, M.J. 1989. Later Quaternary archaeological sequences in Northern Tanzania. Ph.D. Dissertation. University of Illinois, Urbana Champaign.
- Merrick, H.V., Brown, F.H., 1984. Obsidian sources and patterns of source utilization in Kenya and northern Tanzania: some initial findings. *Afr. Archaeol. Rev.* 2 (1), 129–152.

- Menzies, A., Uribe, M., Erazo, F., Ossandon, C., Fonseca, P., 2015. Automated mineralogical analysis of archaeological samples from northern Chile - Case Study II. Ceramics, XIV Congreso Geológico Chileno, La Serena.
- Mollel, G.F., Swisher, C.C., Feigenson, M.D., Carr, M.J., 2008. Geochemical evolution of Ngorongoro Caldera, Northern Tanzania: Implications for crust-magma interaction. *Earth Planet. Sci. Lett.* 271, 337–347.
- Mollel, G.F., Swisher, C.C., 2012. The Ngorongoro volcanic highland and its relationships to volcanic deposits at Olduvai Gorge and East African rift volcanism. *J. Hum. Evol.* 63 (2), 274–283.
- Mturi, A.A., 1986. The Pastoral Neolithic of west Kilimanjaro. *Azania* 2, 53–64.
- Mwitondi, M.S., Bushozi, P.M., 2024. New chronology for Neolithic cultures in the Lake Eyasi Basin, Northern Tanzania. *Zamani: a Journal of Afr. Hist. Stud.* 1 (2), 203–236. <https://doi.org/10.56279/ZJAHS1122>.
- Mwitondi, M.S., Mjandwa, A.S., Bushozi, P.M., 2021. Mollusc shells from Neolithic Contexts in the Lake Eyasi Basin, Northern Tanzania. *Tanzania J. Sci.* 47 (3), 1086–1101.
- Nash, D.J., Ciborowski, T.J.R., Darvill, T., Parker Pearson, M., Ullyott, J.S., Damaschke, M., Evans, J.A., Goderisg, S., Greaney, S., Huggett, J.M., Ixer, R.A., Pirrie, D., Power, M.R., Salge, T., Wilkinson, N. 2021. Petrological and geochemical characterisation of the sarsen stones at Stonehenge. *PLoS ONE*, 16(8): e0254760. <https://doi.org/10.1371/journal.pone.0254760>.
- Odner, K., 1972. Excavations at Narosura, a stone bowl site in the southern Kenya highlands. *Azania* 7, 25–92.
- Ogalde, J.P., Korpisaari, A., Riera-Soto, C., Arriaza, B., Paipa, C., Leyton, P., Campos-Vallette, M., Lara, N., Chacama, J., 2021. Archaeometric analysis of ceramic production in Tiwanaku state (c.500–1000ce): an exploratory study. *Archaeometry* 63, 53–67. <https://doi.org/10.1111/arcm.12597>.
- Ombori, T.L., 2021. Evolution and archaeometrical fabric characterisation of Narosura Pastoral Neolithic Pottery from Luxmunda Site in Mbulu Plateau North-Central Tanzania. Doctoral Thesis. Università degli studi di Ferrara, Italy.
- Ombori, T.L. 2024. Africa, Tropical: Pastoral Neolithic. In: Rehren, T., Nikita, E. (Eds.), Encyclopedia of Archaeology, 2nd Edition, vol. 3, pp. 103–111, London: Academic Press. <https://dx.doi.org/10.1016/B978-0-323-90799-6.00106-3>.
- Peacock, E., Neff, H., Rafferty, J., Meaker, T., 2007. Using laser ablation-inductively coupled plasma-mass spectrometry (LA-ICP-MS) to source shell in shell-tempered pottery: a pilot study from north Mississippi. *Southeast. Archaeol.* 319–329.
- Peterson, S.E., Betancourt, P.P. 2009. Thin-section petrography of ceramic materials. INSTAP archaeological excavation manual 2. INSTAP Academic Press.
- Pirrie, D., Rollinson, G.K., Power, M.R., Webb, J., 2013. Automated forensic soil mineral analysis; testing the potential of lithotyping. *Geol. Soc. Lond. Special Publications* 384, 47–64.
- Prendergast, M.E. 2008. Forager variability and transitions to food production in secondary settings: Kansyore and Pastoral Neolithic economies in East Africa. PhD Dissertation, Harvard University.
- Prendergast, M.E., 2011. Hunters and herders at the periphery: the spread of herding in eastern Africa. In: Jousse, H., Lesur, J., eds., *People and Animals in Holocene Africa: Recent Advances in Archaeozoology*, pp. 43–58. Frankfurt, Africa Magna Verlag.
- Prendergast, M.E., Luque, L., Domínguez-Rodrigo, M., Diez-Martín, F., Mabulla, A.Z., Barba, R., 2007. New excavations at Mumba rockshelter, Tanzania. *J. African Archaeol.* 5 (2), 217–243.
- Prendergast, M.E., Mabulla, A.Z.P., Grillo, K.M., Broderick, L.G., Seitsonen, O., Gidna, A. O., Gifford-Gonzalez, D., 2013. Pastoral Neolithic sites on the southern Mbula Plateau, Tanzania. *Azania: Archaeol. Res. Afr.* <https://doi.org/10.1080/0067270X.2013.841927>.
- Prendergast, M.E., Grillo, K.M., Mabulla, A.Z.P., Wang, H., 2014. New dates for Kansyore and Pastoral Neolithic ceramics in the Eyasi basin, Tanzania. *J. Afr. Archaeol.* 12 (1), 89–98.
- Prendergast, M.E., Janzen, A., Buckley, M., Grillo, K., 2019. Sorting the sheep from the goats in the Pastoral Neolithic: morphological and biomolecular approaches at Luxmunda, Tanzania. *Archaeol. Anthropol. Sci.* 11, 3047–3062.
- Prendergast, M.E., Lipson, M., Sawchuk, E.A., Olalde, I., Ogola, C.A., Rohland, N., Sirak, K.A., et al. 2019b. Ancient DNA reveals a multistep spread of the first herders into Sub-Saharan Africa. *Science*, eaaw6275.
- Quinn, P.S., 2013. Ceramic petrography: the interpretation of archaeological pottery & related artefacts in thin section. *Ceram. Petrogr.* 1–260.
- Quinn, P.S., Ying, Y., Xia, Y., Li, X., Ma, S., Zhang, S., Wilke, D., 2020. Geochemical evidence for the manufacture, logistics and supply-chain management of Emperor Qin Shihuang's Terracotta Army, China. *Archaeometry* 63, 40. <https://doi.org/10.1111/arcn.12613>.
- Quinn, P.S., 2022. Thin section petrography, geochemistry, and scanning electron microscopy of archaeological ceramics. *Archaeopress*.
- Reedy, C., 1994. Thin-section petrography in studies of cultural materials. *J. Am. Inst. Conserv.* 33 (2), 115–129.
- Reedy, C.L. 2008. Thin section petrography of stone and ceramic cultural materials. *Archetype*, London.
- Ring, U., Schwartz, H.L., Bromage, T.G., Sanaane, C., 2005. Kinematic and sedimentological evolution of the Manyara Rift in northern Tanzania, East Africa. *Geol. Mag.* 142, 355–368.
- Robertshaw, P. 2021. Archaeology of Early Pastoralism in East Africa. In Oxford Research Encyclopedia of African History, Oxford University Press, 2021. [DOI: 10.1093/acrefore/978019027734.013.1045](https://doi.org/10.1093/acrefore/978019027734.013.1045).
- Rooney, T., 2020. The Cenozoic magmatism of East Africa: Part III - rifting of the craton. *Lithos* 360, 105390.
- Rubaka, C.C., 2000. Pastoral neolithic settlement and subsistence patterns in the Mang'ola Graben, Tanzania. *Azania* 35 (1), 198–203.
- Schulz, B., Sandmann, D., Gilbricht, S., 2020. SEM-based automated mineralogy and its application in geo- and material sciences. *Minerals* 10, 1004. <https://doi.org/10.3390/min10111004>.
- Šegvić, B., Ugarković, M., Süssberger, A., Ferreiro Mählmann, R., Moscariello, A., 2016. Compositional properties and provenance of Hellenistic pottery from the necropolis of Issa with evidences on the cross-Adriatic and the Mediterranean-scale trade. *Mediterr. Archaeol.* 16, 23–52.
- Storozum, M.J., Goldstein, S.T., Contreras, D.A., Gidna, A.O., Mabulla, A.Z.P., Grillo, K. M., Prendergast, M.E., 2021. The influence of ancient herders on soil development at Luxmunda, Mbula Plateau, Tanzania. *Catena* 204, 105376.
- Thomas, C.M. 1963. Hanang Quarter Degree Sheet 84. Mineral Resources Division, Tanzania.
- Thomas, R.J., Spencer, C., Bushi, A.M., Baglow, N., Boniface, N., de Kock, G., Horstwood, M.S.A., Hollick, L., Jacobs, J., Kajara, S., Kamihanda, G., Key, R.M., Maganga, Z., Mbawala, F., McCourt, W., Momburi, P., Moses, F., Mruma, A., Myambilwa, Y., Roberts, N.M.W., Saidi, H., Nyanda, P., Nyoka, K., Millar, I., 2016. Geochronology of the central Tanzania Craton and its southern and eastern orogenic margins. *Precambrian Res.* 277, 47–67.
- Wandibba, S., 1980. The application of attribute analysis to the study of Later Stone Age/ Neolithic pottery ceramics in Kenya (summary). In: Proceedings of the 8th Panafriican Congress of Prehistory and Quaternary Studies, Nairobi, 5 to 10 September 1977, edited by Leakey and Ogot, 283–85. Nairobi: International Louis Leakey Memorial Institute for African Prehistory.
- Ward, I., Merigot, K., McInnes, B.I.A. 2017. Application of quantitative mineralogical analysis in archaeological micromorphology: a case study from Barrow Is., Western Australia. *Journal of Archaeological Method Theory*, DOI 10.1007/s10816-017-9330-6.
- Ward, I., Moe-Astrup, P., Merigot, K., 2022a. At the water's edge: Micromorphological and quantitative mineral analysis of a submerged Mesolithic shell midden at Hjarnø Sund, Denmark. *J. Archaeol. Sci.* 102, 11–25.
- Ward, I., McDonald, J., Monks, C., Fairweather, J., 2022b. Use of micro-analysis to augment the macro-archaeological investigation of an elevated Holocene shell midden, Dampier Archipelago, NW Australia. *Front. Earth Sci.* 10. <https://doi.org/10.3389/feart.2022.837338>.
- West, M., Ellis, A.T., Potts, P.J., Strelci, C., Vanhoof, C., Wobrauschek, P., 2016. Atomic Spectrometry Update—a review of advances in X-ray fluorescence spectrometry and its applications. *J. Anal. At. Spectrom.* 31 (9), 1706–1755.
- Whitbread, I.K. 1996. Detection and interpretation of preferred orientation in ceramic thin sections. In Higgins, T., Main, P. & Lang, J. (eds.) *Imaging the past: electronic imaging and computer graphics in museums and archaeology*. British Museum, London, Occasional Paper, 114, 173–81.
- Zaitsev, A.N., Marks, M.A.W., Wenzel, T., Spratt, J., Sharygin, V.V., Strekopytov, S., Markl, G., 2012. Mineralogy, geochemistry and petrology of the phonolitic to nephelinic Sadiman volcano, Crater Highlands, Tanzania. *Lithos* 152, 66–83.